First published November 11, 2009; doi:10.1152/ajprenal.00542.2009.

Postobstructive regeneration of kidney is derailed when surge in renal stem cells during course of unilateral ureteral obstruction is halted

H. C. Park,[1,2]* K. Yasuda,[1]* B. Ratliff,[1] A. Stoessel,[3] Y. Sharkovska,[3] I. Yamamoto,[3] J.-F. Jasmin,[4] S. Bachmann,[3] M. P. Lisanti,[4] P. Chander,[1] and M. S. Goligorsky[1]

[1]*Departments of Medicine, Pharmacology, and Pathology, Renal Research Institute, New York Medical College, Valhalla, New York;* [2]*Department of Internal Medicine, Yonsei University Medical College, Seoul, Korea;* [3]*Department of Vegetative Anatomy, Humboldt University Medical School, Berlin, Germany; and* [4]*Departments of Stem Cell Biology and Regenerative Medicine, Cancer Biology, and Medical Oncology and Jefferson Stem Cell Biology and Regenerative Medicine Center, Kimmel Cancer Center, Thomas Jefferson University Medical School, Philadelphia, Pennsylvania*

Submitted 15 September 2009; accepted in final form 10 November 2009

Park HC, Yasuda K, Ratliff B, Stoessel A, Sharkovska Y, Yamamoto I, Jasmin JF, Bachmann S, Lisanti MP, Chander P, Goligorsky MS. Postobstructive regeneration of kidney is derailed when surge in renal stem cells during course of unilateral ureteral obstruction is halted. *Am J Physiol Renal Physiol* 298: F357–F364, 2010. First published November 11, 2009; doi:10.1152/ajprenal.00542.2009.—Unilateral ureteral obstruction (UUO), a model of tubulointerstitial scarring (TIS), has a propensity toward regeneration of renal parenchyma after release of obstruction (RUUO). No information exists on the contribution of stem cells to this process. We performed UUO in FVB/N mice, reversed it after 10 days, and examined kidneys 3 wk after RUUO. UUO resulted in attenuation of renal parenchyma. FACS analysis of endothelial progenitor (EPC), mesenchymal stem (MSC) and hematopoietic stem (HSC) cells obtained from UUO kidneys by collagenase-dispersed single-cell suspension showed significant increase in EPC, MSC, and HSC compared with control. After RUUO cortical parenchyma was nearly restored, and TIS score improved by 3 wk. This reversal process was associated with return of stem cells toward baseline level. When animals were chronically treated with nitric oxide synthase (NOS) inhibitor at a dose that did not induce hypertension but resulted in endothelial dysfunction, TIS scores were not different from control UUO, but EPC number in the kidney decreased significantly; however, parenchymal regeneration in these mice was similar to control. Blockade of CXCR4-mediated engraftment resulted in dramatic worsening of UUO and RUUO. Similar results were obtained in caveolin-1-deficient but not -overexpressing mice, reflecting the fact that activation of CXCR4 occurs in caveolae. The present data show increase in EPC, HSC, and MSC population during UUO and a tendency for these cells to decrease to control level during RUUO. These processes are minimally affected by chronic NOS inhibition. Blockade of CXCR4-stromal cell-derived factor-1 (SDF-1) interaction by AMD3100 or caveolin-1 deficiency significantly reduced the UUO-associated surge in stem cells and prevented parenchymal regeneration after RUUO. We conclude that the surge in stem cell accumulation during UUO is a prerequisite for regeneration of renal parenchyma.

fibrosis; caveolin; AMD3100; mesenchymal stem cells

GLOMERULOSCLEROSIS and tubulointerstitial scarring (TIS)—the main processes governing progression of chronic renal diseases—are well studied and described (3, 7–9, 11, 15). Unilateral ureteral obstruction (UUO) has been consistently utilized as a convenient model of TIS, although this process is much less pronounced in mice than in rats, rabbits, and dogs (5). This model has provided valuable insights into the molecular and cellular mechanisms of TIS progression. Specifically, the role of various subsets of infiltrating leukocytes, hypoxia, angiotensin II, transforming growth factor (TGF)-β, TNF-α, plasminogen activator inhibitor-1, and reactive oxygen species, to name a few, has been established (reviewed in Refs. 3, 5, 7–9, 11, 15). Notwithstanding these advances, significant controversies exist. For instance, the role of stem cells in progression of fibrosis has not been unequivocally established. In a UUO model, Roufosse et al. (17) showed no contribution of bone marrow-derived cells to progression of fibrosis. On the other hand, Yamashita et al. (26) provided evidence that renal resident label-retaining cells undergo transition to myofibroblastic phenotype, thus potentially contributing to the progression of fibrosis. Most recent studies from Weinberg's laboratory (12) have challenged this dogma by demonstrating the ability of epithelial cells that have undergone epithelial-mesenchymal transition to generate stemlike cells. Hence, in general and in this particular case of UUO, the role of stem cells in the progression of TIS remains unresolved.

In this vein, an impressive ability of obstructed shrunken kidneys to structurally regenerate renal parenchyma may be instructive. Clinical experience suggests that the release of UUO (RUUO) not only does not lead to progressive deterioration but is rather associated with improved renal function (2, 16). In experimental RUUO, Cochrane et al. (6) demonstrated partial functional recovery, reduced macrophage infiltration, and decreased proline and collagen content compared with the obstructed state. Could this model provide insights into the role of stem cells during the obstruction, but most importantly, during the postobstructive remodeling of the kidney? Could other factors recently implicated in tipping the balance between fibrosis and regenerative processes, such as the presence of endothelial dysfunction and expression of caveolin-1, modulate the outcome? These questions were addressed in the present study, the results of which demonstrate that preventing the accumulation of hematopoietic stem cells (HSC) and mesenchymal stem cells (MSC) during UUO disrupts post-RUUO regeneration of the renal parenchyma.

MATERIALS AND METHODS

Animal studies. Adult male FVB/N mice (10–12 wk old) were obtained from the Jackson Laboratory (Bar Harbor, ME). Caveolin-1−/− and caveolin-1-overexpressing transgenic male mice of the same age were generated by M. P. Lisanti's laboratory. The animal study protocol was in accordance with the National Institutes of

* H. C. Park and K. Yasuda contributed equally to this work.

Address for reprint requests and other correspondence: M. S. Goligorsky, New York Medical College, Valhalla, NY 10595 (e-mail: michael_goligorsky@nymc.edu).

Health (NIH) *Guide for the Care and Use of Laboratory Animals* and was approved by the Institutional Animal Care and Use Committee. Initially, nine groups of animals were studied (Table 1). Animals in *groups 2*, *3*, *5*, *6*, *8*, and *9* were subjected to left UUO for 10 days. Briefly, animals were anesthetized and placed on a heated surgical pad. The left ureter was visualized via a flank incision and ligated with a vascular clamp (0.4–1.0 mm; Fine Science Tools, Foster City, CA). The UUO was released after 10 days of UUO in *groups 3*, *6*, and *9*, and the kidneys were allowed to recover for 3 wk before death. The right unobstructed kidney served as the control. The animals in *groups 4–6* received N^G-monomethyl-L-arginine (L-NMMA, Axxora, San Diego, CA; 0.3 mg/ml) in drinking water throughout the study period. The animals in *groups 7–9* received AMD3100, a competitive antagonist of CXCR4 (Sigma-Aldrich, St. Louis, MO; 5 mg/kg ip) during the initial 10 days of obstruction, according to the previously published protocol (4). In a separate group of experiments, caveolin-1−/− and caveolin-1-overexpressing transgenic male mice underwent UUO for 10 days.

Assessment of renal morphology and interstitial fibrosis. Kidneys were collected from mice after 10 days of UUO or 3 wk after RUUO for structural analysis ($n = 4–6$ for each group). At harvest, each kidney was washed with saline, blotted dry on gauze, and weighed. Whole kidney weight was expressed as a percentage of body weight determined at the time when mice were euthanized. Midcoronal kidney sections were fixed in 4% paraformaldehyde (PFA) and embedded in paraffin. Paraffin sections (4 μm thick) were stained with hematoxylin and eosin (H & E), periodic acid Schiff, and Masson's trichrome and examined by pathologists blinded to the experimental design. A semiquantitative scale, designed to evaluate the degree of tubulointerstitial injury including tubular atrophy and dilatation (cortex and medulla) and fibrosis (cortex, medulla, papilla, and perivascular area) was used. The tubulointerstitial injury and fibrosis score ranging from 0 to 3 was determined as follows: 0, normal kidney; 1, mild change; 2, moderate change; 3, severe change. Alternatively, kidney sections were stained with Sirius red and scored on the basis of pixel intensity. Changes in renal pelvis and papillary area were also assessed by scores ranging from 0 to 3 with similar criteria. The scores were determined in each section selected at random, and >20 fields were examined under ×100 magnification. The composite tubulointerstitial injury score (TIS) was derived from addition of tubular injury and fibrosis scores. Estimation of cortical thickness was done by measuring the distance from renal capsule to corticomedullary junction.

Isolation of renal cells from whole kidney. For preparation of cell suspensions, individual kidneys from each experimental group were placed in 2 ml of ice-cold RPMI 1640 (Invitrogen, Carlsbad, CA) and minced into small pieces of <1 mm with a sterile scalpel. Digestion of the tissue was performed in collagenase II (Invitrogen) solution (1 mg in 1 ml of RPMI 1640) for 30 min at 37°C in a 5% CO_2 incubator. Cell suspensions were passed through a 35-μm nylon sieve. Repeated digestions were performed until microscopic evaluation showed a suspension of single cells. Finally, cells were washed in PBS-BSA 1% (wt/vol), counted in a Neubauer chamber, and kept on ice in the dark until further analysis. The cell preparation contained intrinsic renal cells and infiltrating cells.

FACS analysis. To quantify the population of endothelial progenitor cells (EPC), HSC, and MSC, 1×10^6 cells from the respective single-cell suspensions were incubated with different primary antibodies for 1 h at 4°C in the dark. The following antibodies were used: FITC-conjugated anti-mouse CD34 (RAM34; eBioscience, San Diego, CA), phycoerythrin (PE)-conjugated anti-mouse Flk-1 (Avas12a1; BD Biosciences, Rockville, MD), PE-conjugated anti-mouse CD150 (eBioscience), FITC-conjugated anti-mouse CD117 (c-Kit; BD Biosciences), monoclonal anti-rat Nestin (Rat-401, Developmental Studies Hybridoma Bank, University of Iowa), and monoclonal anti-vimentin (clone LN-6, Sigma). The cells were permeabilized with 0.2% Triton X-100 for nestin and vimentin staining, and after incubation with nestin and vimentin antibodies cells were incubated with FITC- or Texas red-conjugated goat secondary antibodies (Jackson Immunoresearch, West Grove, PA). In addition, staining was also performed with fluorophore-conjugated antibodies against CD44 and CD29 (both from BD Biosciences). After each incubation step, cells were washed with PBS-BSA 1% (wt/vol) and finally fixed in 1% PFA. Data were acquired with a FACScan cytometer equipped with a 488-nm argon laser and a 635-nm red diode laser and analyzed with CellQuest software (Becton Dickinson). The setup of the FACScan was performed with unstained and secondary antibody-stained cells. For quantification of EPC and HSC, the number of CD34/Flk-1 and CD150/c-Kit double-positive cells, respectively, within the monocytic cell population was counted. MSC were quantified by counting cells positive for nestin, vimentin, or CD44 and CD29.

Statistical analyses. Values are expressed as means ± SE. For comparison between two groups, an unpaired *t*-test or nonparametric Mann-Whitney *U*-test was performed. For more than two groups, a Kruskal-Wallis test was used. A P value <0.05 was considered indicative of a significant difference.

RESULTS

Renal morphology and histopathological scoring. Ten days of UUO resulted in a significant shrinkage of the obstructed kidney (Table 1), as judged by the ratio of kidney weight to body weight (KW/BW) compared with control nonobstructed kidney (CK). RUUO resulted in a remarkable restoration of kidney weight within 21 days, in accord with previous observations by Cochrane et al. (6).

Table 1. *Kidney weight and renal cortical thickness after UUO and 3 wk after relief of UUO*

Group	*n*	Treatment	Percent Kidney Weight, %body wt		Cortical Thickness, mm	
			Contr	Obstr	Contr	Obstr
1	4	Unilateral control	0.91 ± 0.02		1,244 ± 18	
2	6	10-day UUO	1.02 ± 0.05	0.77 ± 0.03*	1,344 ± 95	900 ± 45*
3	4	10-day UUO +3-wk relief	0.86 ± 0.04	0.84 ± 0.04	1,280 ± 110	1,171 ± 77
4	4	L-NMMA only	0.83 ± 0.07		1,217 ± 118	
5	4	10-day UUO + L-NMMA	0.77 ± 0.07	0.74 ± 0.03*	1,250 ± 92	964 ± 26*
6	4	10-day UUO +3 wk + L-NMMA	0.71 ± 0.02	0.71 ± 0.01	1,312 ± 38	1,166 ± 48
7	4	AMD3100 only	0.80 ± 0.03		1,207 ± 49	
8	6	10-day UUO + AMD3100	0.78 ± 0.04	0.70 ± 0.02*	1,214 ± 35	971 ± 67*
9	4	10-day UUO +3 wk + AMD3100	1.16 ± 0.01*	0.39 ± 0.07*	1,407 ± 37*	507 ± 39*

Values are means ± SE for *n* mice. UUO, unilateral ureteral obstruction; Contr, contralateral nonobstructed kidney; Obstr, UUO; L-NMMA, N^G-monomethyl-L-arginine. *$P < 0.05$ compared with control kidney.

Renal morphology and tubulointerstitial damage were examined with H & E staining and Masson's trichrome or Sirius red, respectively. The CK showed normal histoarchitecture, with distinct cortex, medulla, and renal papilla. In contrast, UUO kidney displayed conspicuous dilated proximal tubules and increased collagen deposition in tubulointerstitial areas (Fig. 1). UUO was associated with a marked attenuation of renal papilla and thinning of outer medulla and cortex (25% reduction from CK). However, after 3 wk of RUUO, the cortex and the medulla showed a remarkable restoration of renal parenchyma. Cortical thickness was recovered almost to control level (14% increased from UUO).

Stem cell accumulation during UUO. One of the possible mechanisms to account for the rapid restoration of the renal parenchyma after the relief of obstruction could be stem cell dependent. To determine the possible participation of stem cells during UUO or during regenerative processes after RUUO, we performed flow cytometric analysis of cells isolated from whole kidneys. Compared with CK, flow cytometric analysis of renal cells isolated from UUO kidney demonstrated a significant increase in CD34/Flk-1 (3-fold vs. control; approximate number of these cells in the kidney averages 3×10^4 in control and 9.9×10^4 in UUO) and CD150/c-kit (9-fold vs. control; approximate number of these cells in the kidney averages 21×10^4 in control and 134×10^4 in UUO) double-positive cells, indicative of EPC and HSC accumulation, respectively. Nestin (4-fold vs. control)- and vimentin (15-fold vs. control)-positive cells, as well as CD29/CD44 (5-fold vs. control; approximate number of these cells in the kidney averages 13×10^4 in control and 78×10^4 in UUO) double-positive cells were also significantly increased after UUO, suggesting an increase in cells of the mesenchymal lineage during UUO. Ten-day UUO followed by 3 wk of RUUO was characterized by a significant drop in EPC, HSC, and MSC almost to baseline control levels (Figs. 2 and 3).

Effect of nitric oxide synthase inhibition on natural course of UUO and its relief. There is accumulating, albeit controversial, evidence linking stem cell mobilization with nitric oxide synthase (NOS) function (1, 13). Therefore, we addressed the next question: Does inhibition of NOS with nonhypertensinogenic doses of L-NMMA affect stem cell recruitment by the obstructed kidney? To avoid any contribution of elevation in blood pressure to the results of UUO, we employed subpressor doses of L-NMMA that have been shown to induce a mild endothelial dysfunction but no proteinuria or other functional changes in the kidney (19). UUO kidneys from L-NMMA-treated mice showed a similar reduction of KW/BW compared with CK or RUUO kidney of nontreated mice. The data demonstrated that L-NMMA-treated CK showed normal histoarchitecture except for a slight increase in perivascular fibrosis and UUO kidneys displayed marked tubular dilatation with increased interstitial collagen deposition. After 3 wk of RUUO, L-NMMA-treated kidneys showed a significant restoration of tubular dilatation and decline in interstitial collagen deposition (Fig. 1, *D–F*).

Subpressor doses of L-NMMA (0.3 mg/ml) also showed a similar pattern of increase in EPC, HSC, and MSC during UUO. Such increase in EPC, HSC, and nestin- and vimentin-positive cells during UUO was attenuated after RUUO, as in the control group. Of interest, the increase in EPC was significantly less pronounced in the L-NMMA-treated mice compared with the nontreated control group. On the other hand, the CD150/c-kit-positive cells and nestin- and vimentin-positive cells showed comparable increase after UUO in control and L-NMMA-treated mice. These data indicate that subpressor doses of L-NMMA, previously shown to be associated with mild endothelial dysfunction (19), did not significantly alter the course of UUO or RUUO, despite the curtailed surge in renal EPC. Hence, it appears that mild nitric oxide deficiency does not alter fibrotic and regenerative processes at least in the present experimental setting (Fig. 3).

Blockade of stem cell recruitment to obstructed kidney and its effect on postobstructive regeneration. To elucidate the role accumulating stem cells during UUO play in post-RUUO regeneration, we next attempted to prevent engraftment of kidney by stem/progenitor cells. Blockade of CXCR4 receptor by AMD3100 treatment significantly blunted the increase of EPC, HSC, and MSC during UUO (*group 2* vs. *group 8*), suggesting possible attenuation of stem cell engraftment in UUO kidney. Late increase in EPC, HSC, and MSC was noted after discontinuation of AMD3100 treatment in RUUO kidney (Fig. 4).

AMD3100-treated mice showed a significant reduction of KW/BW in UUO kidneys compared with CK. Furthermore,

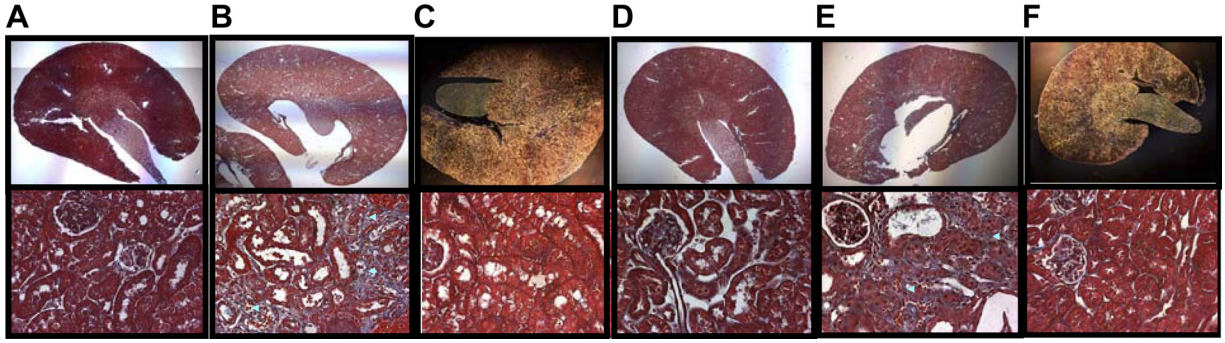

Fig. 1. Representative images of the kidneys obtained from mice with unilateral ureteral obstruction (UUO) and after its release (RUUO) *A*: control nonobstructed kidney showing normal distinct cortex, medulla, and renal papilla without interstitial fibrosis. *B*: marked attenuation of renal papilla and outer medullary area with thinning of renal cortex. Markedly dilated tubules and increased collagen deposition are seen with 10-day UUO. *C*: mild dilatation of tubules with partial restoration of renal parenchyma are noted 3 wk after RUUO. *D*: N^G-monomethyl-L-arginine (L-NMMA)-treated control mice show normal histoarchitecture except for a minimal increase in perivascular fibrosis. *E*: UUO on the L-NMMA background demonstrates marked tubular dilatation with increased collagen deposition. *F*: RUUO on the L-NMMA background displays significant restoration of histoarchitecture and reduced collagen deposition. Masson's trichrome stain: *top*, panoramic views at magnification ×40; *bottom*, magnification ×400. $n = 4–6$ in each group.

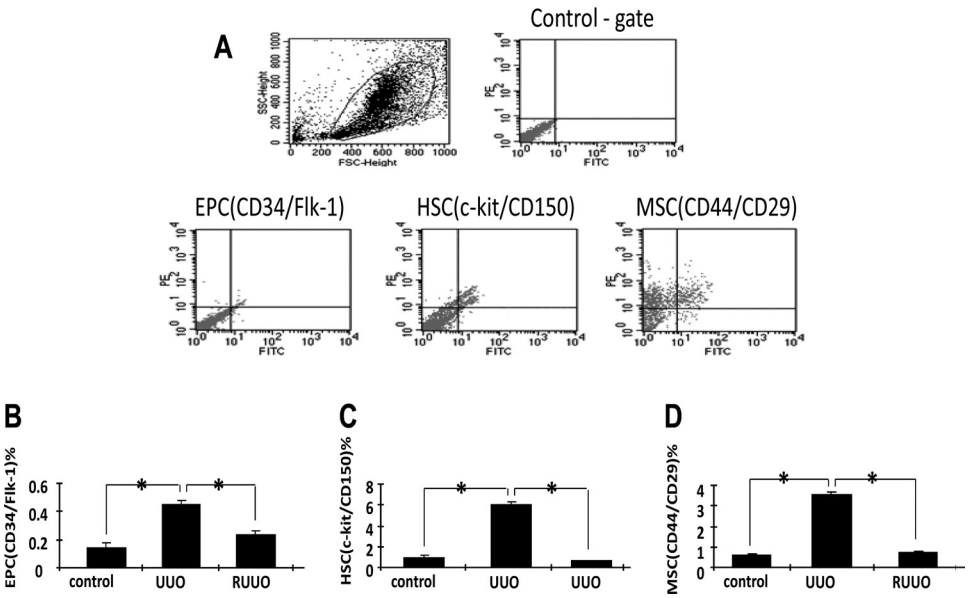

Fig. 2. Typical FACS gating parameters and distribution of cells of interest (*A*) and bar diagrams summarizing the proportion of CD34+/Flk-1+ [endothelial progenitor (EPC); *B*], c-Kit+/CD150+ [hematopoietic stem (HSC); *C*], and CD44+/CD29+ [mesenchymal stem (MSC); *D*] cells. *$P < 0.05$.

RUUO kidneys showed further decrease in KW/BW compared with control kidneys (Table 1). CK in AMD3100-treated mice showed a near normal histoarchitecture, whereas UUO kidney showed a significant increase in tubular injury and interstitial fibrosis that was accompanied by marked attenuation of renal papilla with thinning of outer medulla and cortex (Table 2). In contrast to nontreated control mice subjected to the analogous treatments, 3 wk of RUUO in AMD3100-treated mice showed further aggravation in the loss of renal parenchyma with persisting papillary attenuation and renal pelvis dilatation (Fig. 5).

Role of caveolin-1 expression level in progression of fibrosis. Another way to manipulate stem cell engraftment of the kidney is through regulation of caveolin-1 expression. Caveolin-1 expression is a prerequisite for stem cell engraftment because CXCR4 dimerization induced by stromal cell-derived factor-1 (SDF-1) occurs in caveolar lipid-rich domains (24). It has been shown that incorporation of CXCR4 into membrane lipid rafts is necessary for SDF-1-induced homing of HSC and EPC (25). These data raised the question of the role played by CXCR4-SDF-1 interaction in the observed surge of stem cells in the obstructed kidney.

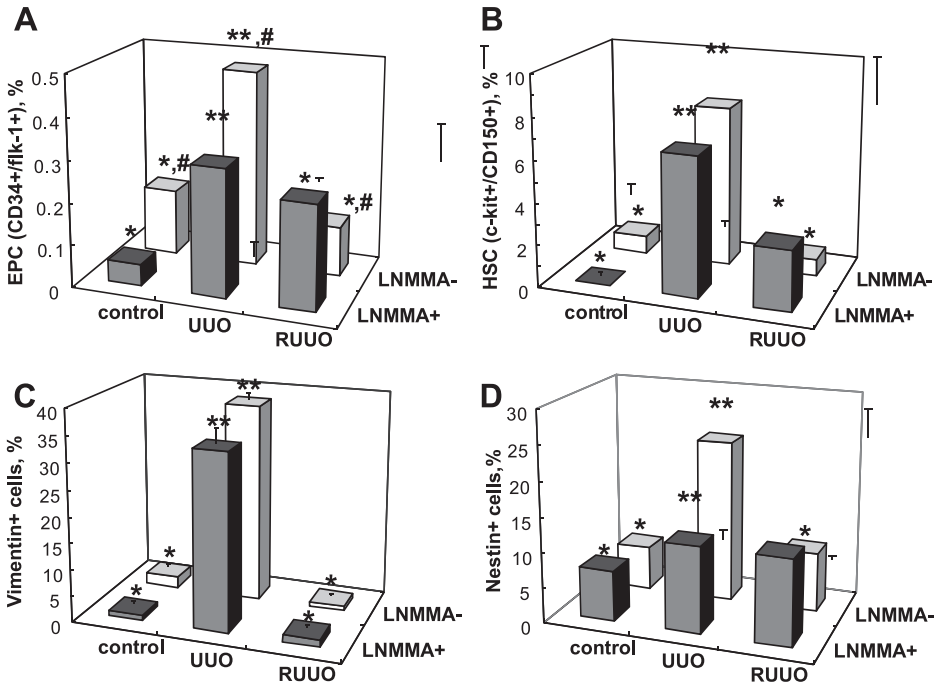

Fig. 3. Stem cell mobilization during UUO and RUUO. Flow cytometric analysis of single-cell suspensions prepared from kidneys of control, UUO, and RUUO in naive and L-NMMA-treated mice as described in MATERIALS AND METHODS. Compared with control, UUO kidneys demonstrated a significant increase in EPC (*A*), HSC (*B*), and CML (*C*, *D*), and this surge in stem cells decreased almost back to baseline 3 wk after RUUO. UUO in mice treated with nonpressor dose of L-NMMA also showed similar surge of stem cells. However, the increase in EPC was less pronounced compared with the control group. Values are means ± SE; $n = 4–8$ in each group.

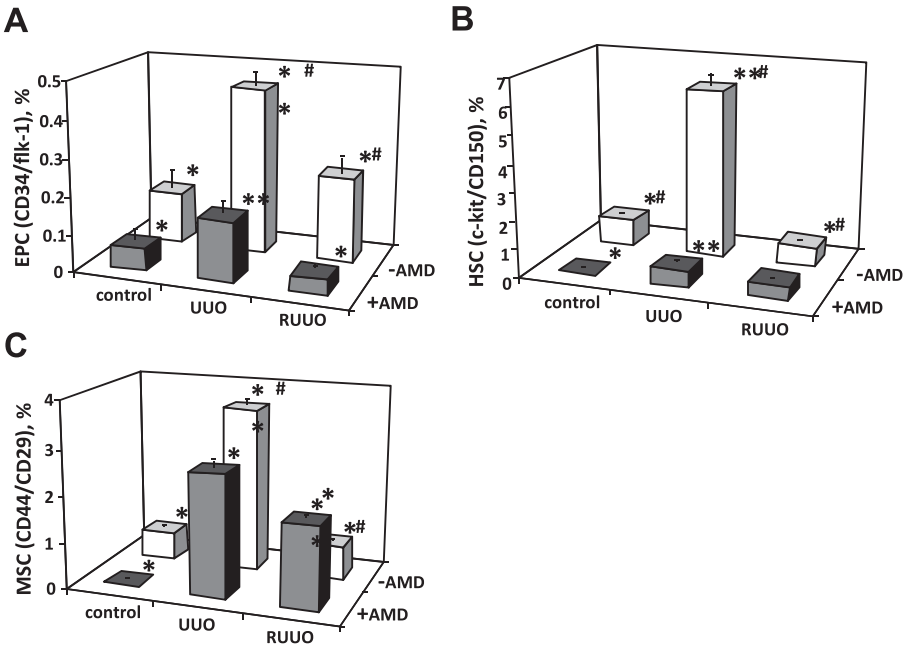

Fig. 4. Effect of AMD3100 on stem cell mobilization in control, UUO, and RUUO kidneys. AMD3100 treatment significantly attenuated the increase of EPC (*A*), HSC (*B*), and MSC (*C*) during UUO, suggesting blunting of stem cell engraftment in the kidney. Late increase in EPC, HSC, and CML was noted after discontinuation of AMD3100 treatment in RUUO kidney. Values are means ± SE; $n = 4–6$ in each group. $^{*}P < 0.05$ vs. UUO; $^{**}P < 0.05$ vs. control; $^{\#}P < 0.05$ vs. AMD3100-treated mice.

To address this question, we examined the course of UUO in caveolin-1-deficient and caveolin-1-overexpressing mice. Genetic manipulation of caveolin-1 expression level resulted in strikingly divergent responses to UUO. In caveolin-1−/− mice, the degree of developing fibrosis was dramatically increased compared with wild-type and caveolin-1-overexpressing transgenic animals (Fig. 6). At the level of the microvasculature, however, the highest increase in neointimal formation, as judged by the media-to-lumen ratio, was detected in caveolin-1-overexpressing mice (Fig. 7).

The abundance of stem cells in the kidney was examined next. As shown in Fig. 8, only the postobstructive surge of MSC in the kidney was dramatically curtailed in caveolin-1−/− mice, whereas EPC and HSC, although slightly reduced, did not change significantly. The fact that caveolin-1 deficiency was associated with the worsening of interstitial fibrosis and reduction in renal MSC, compared with obstruction in wild-type mice, suggests that accumulation of MSC does not necessarily lead to aggravation of fibrosis; rather it is the reduction of their surge that is associated with worsening of interstitial fibrosis.

DISCUSSION

UUO is associated with progressive renal fibrosis and scarring and a decline in renal function. RUUO is characterized by a variable recovery of renal function and structural repair of renal parenchyma. Although numerous studies have examined the events that lead to renal fibrosis, less is known about the inherent mechanisms that promote tissue remodeling and regeneration. A mouse model of UUO and RUUO that results in the development of renal fibrosis and loss of parenchyma followed by resolution of renal injury and regeneration of renal parenchyma was established by Cochrane et al. (6) and reexamined here, along with several recently discovered modulators of fibrosis and/or regeneration.

The obstructed kidney from 10-day UUO demonstrated profound ablation of renal cortex and outer medulla and was accompanied by marked increase in EPC, HSC, and MSC in the renal parenchyma. After 3-wk RUUO, cortical parenchymal thickness was nearly restored, along with decrease of EPC, HSC, and vimentin- or nestin-positive cells. Treatment with AMD3100, a specific antagonist of CXCR4, markedly attenuated observed stem cell mobilization during 10-day UUO and was associated with the failure to regenerate renal parenchyma after 3-wk RUUO. Flow cytometric analysis of renal parenchymal cells in AMD3100-treated mice after 3-wk RUUO showed delayed marked increase in EPC, HSC, and vimentin- and nestin-positive, as well as CD29- and CD44-positive cells. These results suggest that a wave of stem cell accumulation in the kidney during the period of obstruction, but not after its

Table 2. *Tubulointerstitial injury score*

Group	*n*	TIS	Tubular Injury	Fibrosis Score	Pelvis Dilatation	Papillary Attenuation
1	4	<0.01	<0.01	<0.01		
2	6	3.90 ± 0.87	2.34 ± 0.53	1.56 ± 0.34	2.89 ± 0.07	2.56 ± 0.17
3	4	0.31 ± 0.22	<0.01	0.31 ± 0.22	0.50 ± 0.29	<0.01
4	4	0.08	<0.01	0.08		
5	4	4.07 ± 1.35	1.78 ± 0.49	2.29 ± 0.86	2.25 ± 0.31	2.19 ± 0.37
6	4	0.63 ± 0.38	<0.01	0.63 ± 0.38	1.25 ± 0.25	1.25 ± 0.25
7	4	0.1 ± 0.18	<0.01	0.1 ± 0.18		
8	6	3.63 ± 1.2	1.84 ± 0.62	1.79 ± 0.58	2.14 ± 0.49	2.13 ± 0.44
9	4	5.17 ± 0.83	2.78 ± 0.35	2.39 ± 0.48	2.86 ± 0.24	2.71 ± 0.41

Values are means ± SE for *n* mice. TIS, composite tubular injury score (= tubular injury + fibrosis score).

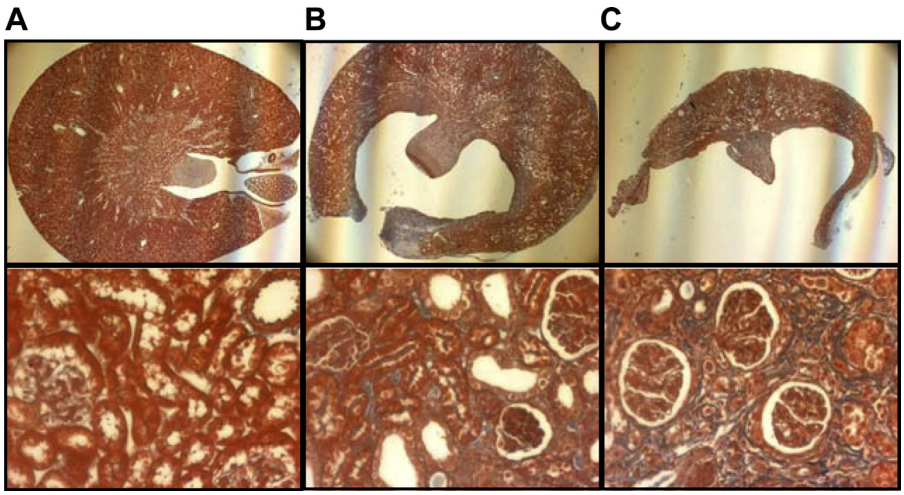

Fig. 5. Effect of AMD3100 on postobstructive kidney regeneration: representative images of kidneys obtained from mice with 10-day UUO and 3 wk after its release. AMD3100-treated control mice kidney appears grossly normal (*A*). UUO in AMD3100 treated mice demonstrated marked tubular dilatation with increased collagen deposition. Moreover, marked attenuation of renal papilla and thinning of outer medullar and cortical areas are noted (*B*). After 3 wk of RUUO, AMD3100-treated kidneys display further shrinkage of renal parenchyma, especially the outer medulla and the cortex (*C*). Masson's trichrome stain: *top*, panoramic views at magnification ×40; *bottom*, magnification ×400; $n = 4–6$ in each group.

release, may serve as a mechanism of renal structural repair following RUUO.

Owing to the fact that all studied cells, EPC, HSC, and MSC, showed a surge in the obstructed kidneys, it is difficult to dissociate the contribution of each cell type to the postrelief structural recovery. In this vein, the results of L-NMMA pretreatment may shed some light. Under these experimental conditions, only the surge in EPC was found to be inhibited, whereas the numbers of HSC and MSC residing in the obstructed kidneys were not different from nontreated controls. The fact that this did not affect the regenerative outcome after the release of obstruction may be indicative of the leading role played by HSC and/or MSC in the positive remodeling. It must be acknowledged, however, that a two-parameter assignment of cells to different stem cell populations is tenuous. Despite the fact that traditional markers have been utilized in this study, some overlap with nonstem cells is inevitable and interpretation of findings requires caution.

Prior experience with stem cell mobilization or transplantation in UUO brought about conflicting results. Stem cell factor (SCF)- or granulocyte-colony stimulating factor (G-CSF)-induced mobilization of bone marrow stem cells did not reduce tubulointerstitial fibrosis in UUO (20). This finding may be difficult to interpret as it could represent the net result of opposing trends due to the multicellular nature of mobilizing effects elicited by either of these agents, which could have canceled each other. For instance, increased influx of classically activated macrophages could potentially aggravate fibrosis, in fact reversing any possible beneficial effect observed upon macrophage depletion in UUO (21). In accord with our findings, however, label-retaining cells were found in increased numbers after UUO (26), where they reportedly participated in epithelial-mesenchymal transition. The role played by these cells in postrelief remodeling and tissue regeneration was not studied. Our data suggest that the accumulated stem cells could have participated in this process. This conclusion is based on

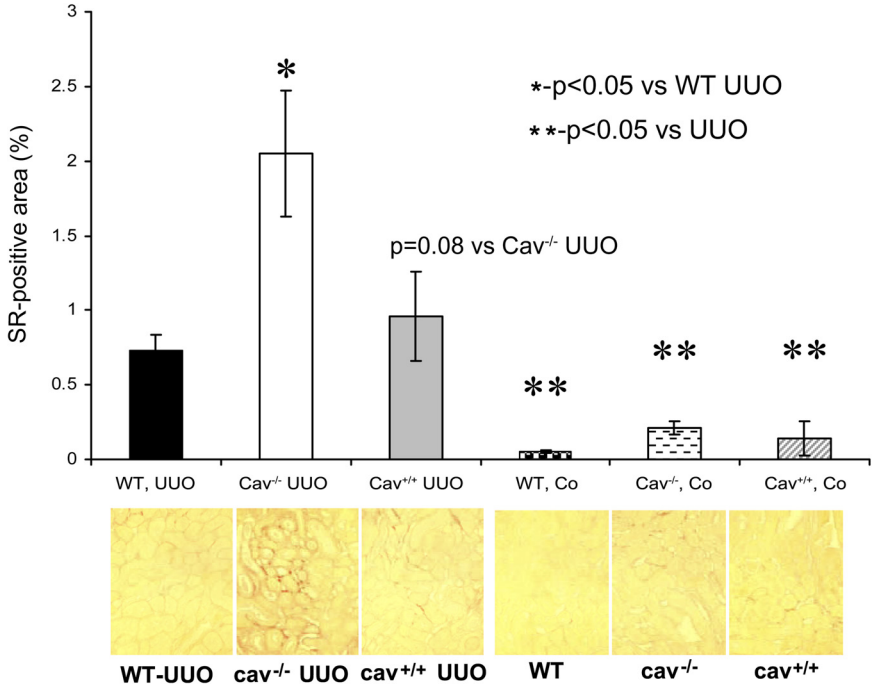

Fig. 6. Fibrosis is prevalent in caveolin-1−/− obstructed kidneys. Quantitative assessment of the degree of fibrosis, as assessed with Sirius red (SR) staining, in Cav-1−/− and Cav-1-overexpressing mice compared with wild-type (WT) counterparts subjected to UUO (*top*) and representative images of obstructed kidneys (*bottom*). Values are means ± SE; $n = 4–6$.

the demonstration of halted and even reversed regeneration in mice treated with AMD3100, which curtailed the accumulation of stem cells in the kidney, possibly via the reduced engraftment. Indeed, we have no data to support or reject the possibility of engraftment versus proliferation of resident stem cells in the obstructed kidney; such an analysis would require cell fate tracing experiments. EPC did not appear to be of critical importance for the regenerative processes, insofar as prevention of their accumulation in the obstructed kidney did not palpably affect the postrelief outcome.

It can be argued that the detectable population of CD34-positive/Flk-1-positive cells may incorporate mature endothelial cells. Unfortunately, this is an unavoidable limitation of the techniques used. However, considering the opposite trends in the shrinking size of population of vascular endothelial cells in the obstructed kidney vis-à-vis the growing number of detectable CD34+/Flk-1+ cells, it is reasonable to assume that the difference reflects the increased contribution by EPC.

The data obtained in caveolin-1 knockout and transgenic mice may emphasize the contribution of enhanced stem cell mobilization and impaired engraftment: Apart from its role in the activation of CXCR4, caveolin-1 may also play an important role in stem cell mobilization. Sbaa et al. (18) have demonstrated that neovascularization in Cav-1−/− mice impaired because of the defective mobilization of EPC from the bone marrow after stimulation with SDF-1. This was due to the blockade of CXCR4 internalization in the absence of caveolin-1. At the same time, adhesion of Cav-1−/− EPC to SDF-1-presenting endothelial cells was enhanced, a property that could be reproduced in wild-type mice by small interfering RNA inhibition of caveolin-1 expression. These data emphasize the existing caveolin-dependent dualism in SDF-1-induced actions on CXCR4: Caveolin-1 deficiency causes both reduced mobilization and enhanced homing, a paradox that requires further in-depth studies. Using fluorescence resonance energy transfer, Toth et al. (22) demonstrated that SDF-1 enhanced CXCR4 receptor dimerization, an effect that was inhibited by the CXCR4 antagonist AMD3100. In a model of vascular injury, however, caveolin-1 deficiency enhances neointimal formation (10). Caveolin-1 deficiency has been found to increase cell proliferation and collagen synthesis, thus leading to myocardial hypertrophy and pulmonary hypertension; both were normalized in Cav-1−/− mice by reexpressing caveolin-1 in endothelial cells (14). In accord with this, administration of caveolin-1 scaffolding domain peptide (Cavtratin) affords an antifibrotic effect in lung injury (23).

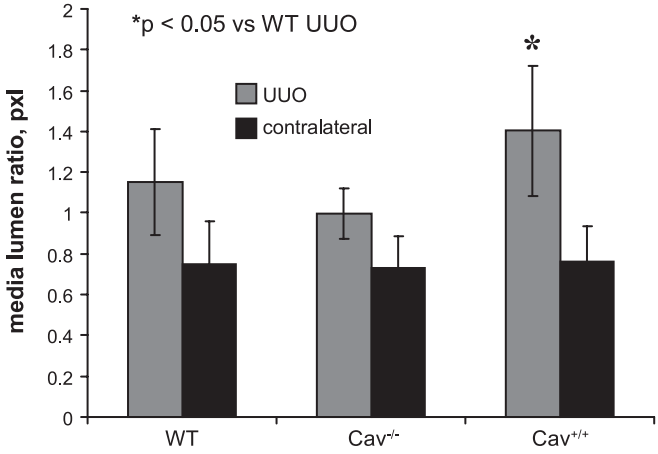

Fig. 7. Media-to-lumen ratio in renal arterioles of Cav-1−/−, Cav-1-overexpressing, and wild-type littermates after UUO. Note that Cav-1-overexpressing mice respond to UUO with the highest increase of media-to-lumen ratio. Values are means ± SE; $n = 4–6$ in each group.

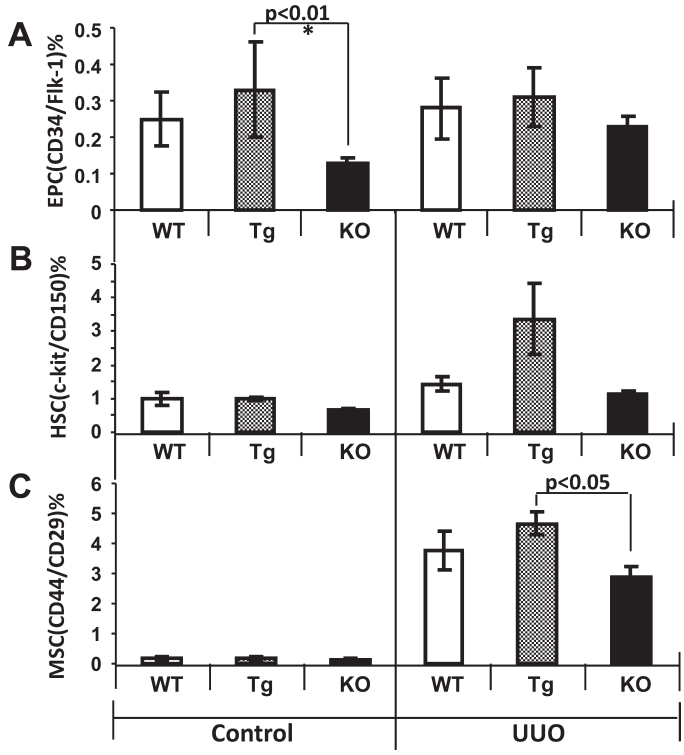

Fig. 8. Stem cells in obstructed kidneys of Cav-1−/− and transgenic mice: EPC (*A*), HSC (B), and MSC (*C*) after 10 days of UUO. Note that the postobstructive surge of MSC in the kidney was dramatically curtailed in Cav-1−/− mice, whereas EPC and HSC, although slightly reduced, did not change significantly. Values are means ± SE; $n = 4–6$ in each group. WT, control; Tg, transgenic; KO, knockout.

In addition, our data suggest that the timing of stem cell accumulation in the renal parenchyma of the obstructed kidney is of essence: Despite the fact that cells reaccumulate after the relief of obstruction and cessation of AMD treatment, regeneration does not occur and fibrosis progresses.

In conclusion, the data presented here extend previous observations by Cochrane et al. (6), as well as the existing clinical experience on the regenerative capacity of the kidney after obstruction has been relieved. One of the proposed mechanisms for positive kidney remodeling under these conditions has been identified here as the accumulation of stem cells and the derailment of parenchymal regeneration when the surge in stem cells was halted. The data presented allow us to rule out the major role of EPC in this process and suggest the potential contribution of MSC and HSC, although they do not distinguish between them.

ACKNOWLEDGMENTS

Authors are grateful to Dr. J. Ni for the initial help with FACS analysis.

GRANTS

These studies were supported in part by National Institute of Diabetes and Digestive and Kidney Diseases Grants DK-52783, DK-45462, and DK-54602

(M. S. Goligorsky) and Westchester Artificial Kidney Foundation and Faculty Research Grant of Yonsei University College of Medicine (H. C. Park, 6-2008-265, 280).

DISCLOSURES

No conflicts of interest are declared by the authors.

REFERENCES

1. **Aicher A, Heeschen C, Dimmeler S.** The role of NOS3 in stem cell mobilization. *Trends Mol Med* 10: 421–425, 2004.
2. **Albani JM, Desai MM, Gill IS, Streem SB.** Repair of adult ureteropelvic junction obstruction in the solitary kidney: effect on renal function. *Urology* 68: 718–722, 2006.
3. **Brenner BM.** Remission of renal disease: recounting the challenge, acquiring the goal. *J Clin Invest* 110: 1753–1758, 2002.
4. **Broxmeyer HE, Orschell CM, Clapp DW, Hangoc G, Cooper S, Plett PA, Liles WC, Li X, Graham-Evans B, Campbell TB, Calandra G, Bridger G, Dale DC, Srour EF.** Rapid mobilization of murine and human hematopoietic stem and progenitor cells with AMD3100, a CXCR4 antagonist. *J Exp Med* 201: 1307–1318, 2005.
5. **Chevalier RL, Forbes MS, Thornhill BA.** Ureteral obstruction as a model of renal interstitial fibrosis and obstructive nephropathy. *Kidney Int* 75: 1145–1152, 2009.
6. **Cochrane AL, Kett MM, Samuel CS, Campanale NV, Anderson WP, Hume DA, Little MH, Bertram JF, Ricardo SD.** Renal structural and functional repair in a mouse model of reversal of ureteral obstruction. *J Am Soc Nephrol* 16: 3623–3630, 2005.
7. **Eddy AA.** Molecular insights into renal interstitial fibrosis. *J Am Soc Nephrol* 7: 2495–2508, 1996.
8. **Eitner F, Floege J.** Novel insights into renal fibrosis. *Curr Opin Nephrol Hypertens* 12: 227–232, 2003.
9. **Fogo AB.** Renal fibrosis and the renin-angiotensin system. *Adv Nephrol Necker Hosp* 31: 69–87, 2001.
10. **Hassan GS, Jasmin JF, Schubert W, Frank PG, Lisanti MP.** Caveolin-1 deficiency stimulates neointima formation during vascular injury. *Biochemistry* 43: 8312–8321, 2004.
11. **Lan HY.** Tubular epithelial-myofibroblast transdifferentiation mechanisms in proximal tubule cells. *Curr Opin Nephrol Hypertens* 12: 25–29, 2003.
12. **Mani SA, Guo W, Liao MJ, Eaton EN, Ayyanan A, Zhou AY, Brooks M, Reinhard F, Zhang CC, Shipitsin M, Campbell LL, Polyak K, Brisken C, Yang J, Weinberg RA.** The epithelial-mesenchymal transition generates cells with properties of stem cells. *Cell* 133: 704–715, 2008.
13. **Michurina T, Krasnov P, Balazs A, Nakaya N, Vasilieva T, Kuzin B, Khrushchov N, Mulligan RC, Enikolopov G.** Nitric oxide is a regulator of hematopoietic stem cell activity. *Mol Ther* 10: 241–248, 2004.
14. **Murata T, Lin MI, Huang Y, Yu J, Bauer PM, Giordano FJ, Sessa WC.** Reexpression of caveolin-1 in endothelium rescues the vascular, cardiac, and pulmonary defects in global caveolin-1 knockout mice. *J Exp Med* 204: 2373–2382, 2007.
15. **Nakagawa T, Kang DH, Ohashi R, Suga S, Herrera-Acosta J, Rodriguez-Iturbe B, Johnson RJ.** Tubulointerstitial disease: role of ischemia and microvascular disease. *Curr Opin Nephrol Hypertens* 12: 233–241, 2003.
16. **Ravanan R, Tomson CR.** Natural history of postobstructive nephropathy: a single-center retrospective study. *Nephron Clin Pract* 105: c165–c170, 2007.
17. **Roufosse C, Bou-Gharios G, Prodromidi E, Alexakis C, Jeffery R, Khan S, Otto WR, Alter J, Poulsom R, Cook HT.** Bone marrow-derived cells do not contribute significantly to collagen I synthesis in a murine model of renal fibrosis. *J Am Soc Nephrol* 17: 775–782, 2006.
18. **Sbaa E, Dewever J, Martinive P, Bouzin C, Frerart F, Balligand JL, Dessy C, Feron O.** Caveolin plays a central role in endothelial progenitor cell mobilization and homing in SDF-1-driven postischemic vasculogenesis. *Circ Res* 98: 1219–1227, 2006.
19. **Stoessel A, Paliege A, Theilig F, Addabbo F, Ratliff B, Waschke J, Patschan D, Goligorsky MS, Bachmann S.** Indolent course of tubulointerstitial disease in a mouse model of subpressor, low-dose nitric oxide synthase inhibition. *Am J Physiol Renal Physiol* 295: F717–F725, 2008.
20. **Stokman G, Leemans JC, Stroo I, Hoedemaeker I, Claessen N, Teske GJ, Weening JJ, Florquin S.** Enhanced mobilization of bone marrow cells does not ameliorate renal fibrosis. *Nephrol Dial Transplant* 23: 483–491, 2008.
21. **Sung SA, Jo SK, Cho WY, Won NH, Kim HK.** Reduction of renal fibrosis as a result of liposome encapsulated clodronate induced macrophage depletion after unilateral ureteral obstruction in rats. *Nephron Exp Nephrol* 105: e1–e9, 2007.
22. **Toth PT, Ren D, Miller RJ.** Regulation of CXCR4 receptor dimerization by the chemokine SDF-1alpha and the HIV-1 coat protein gp120: a fluorescence resonance energy transfer (FRET) study. *J Pharmacol Exp Ther* 310: 8–17, 2004.
23. **Tourkina E, Richard M, Gooz P, Bonner M, Pannu J, Harley R, Bernatchez PN, Sessa WC, Silver RM, Hoffman S.** Antifibrotic properties of caveolin-1 scaffolding domain in vitro and in vivo. *Am J Physiol Lung Cell Mol Physiol* 294: L843–L861, 2008.
24. **van Buul JD, Voermans C, van Gelderen J, Anthony EC, van der Schoot CE, Hordijk PL.** Leukocyte-endothelium interaction promotes SDF-1-dependent polarization of CXCR4. *J Biol Chem* 278: 30302–30310, 2003.
25. **Wysoczynski M, Reca R, Ratajczak J, Kucia M, Shirvaikar N, Honczarenko M, Mills M, Wanzeck J, Janowska-Wieczorek A, Ratajczak MZ.** Incorporation of CXCR4 into membrane lipid rafts primes homing-related responses of hematopoietic stem/progenitor cells to an SDF-1 gradient. *Blood* 105: 40–48, 2005.
26. **Yamashita S, Maeshima A, Nojima Y.** Involvement of renal progenitor tubular cells in epithelial-to-mesenchymal transition in fibrotic rat kidneys. *J Am Soc Nephrol* 16: 2044–2051, 2005.